Vibration Tailoring of Advanced Composite Lifting Surfaces

Terrence A. Weisshaar*
Purdue University, West Lafayette, Indiana
and
Brian L. Foist†
Northrop Corporation, Pico Rivera, California

This paper discusses the free-vibration characteristics of directionally stiffened, laminated composite beam-like structures such as high-aspect-ratio lifting surfaces. A bounded nondimensional parameter, ψ, is defined to describe the degree of elastic coupling between bending curvature and twist rate for a laminated beam. In addition, three different stiffness models commonly used to model laminated beam/tube deformation are described and compared. Using one of these models, the ability of the laminate design to control mode shape or node line characteristics is illustrated for a cross-coupled laminated cantilever beam. Finally, the effect of the nondimensional cross-coupling parameter, ψ, on cantilever beam free-vibration node line positions and frequencies is illustrated, independent of a specific laminate design.

Introduction

An extensive amount of literature related to the static and dynamic effects of bend/twist deformation coupling is available. References 1-9 are significant examples of such literature. As early as 1928, it was recognized that crystalline materials displayed anisotropic behavior with respect to arbitrarily oriented axes. Because of this anisotropy, the application of either a bending or twisting moment by itself produced both bending and twisting of a material specimen. Such coupled behavior (or failure to account for this effect) can produce incorrect estimates of material properties when specimens are used in dynamic or static tests.[2]

Ritchie and Rosinger[6] have pointed out other effects related to bend/twist coupling of beam-like specimens. In particular, deformation coupling complicates the interpretation of test results because of problems associated with the identification and categorization of vibration modes. Analytical and experimental results for both free-free and cantilevered plates of high aspect ratio have been developed by a number of authors[3-9] to illustrate the effects of anistropy on a vibration mode shape.

The effects of controlled, as opposed to accidental, anisotropy have only recently been of interest to the aeronautical community. This interest is due in large part to the positive benefits of structural optimization and aeroelastic tailoring upon aircraft design (cf., Ref. 10). The present paper focuses upon a number of the same phenomena presented by the references cited previously. However, the emphasis of the present study is upon analytical modeling and structural dynamic behavior oriented toward aeroelastic tailoring analyses.

This paper will discuss and illustrate several structural dynamic effects that may be obtained by intentionally coupling together the structural bending and torsional flexibilities of a slender, beam-like structure. Topics to be considered include: modeling of cross-sectional stiffness properties of a beam-like structure and the effect of internal chordwise structural construction or restraints, such as may be provided by ribs, upon stiffness cross-coupling; the effects of stiffness cross-coupling on beam free-vibration mode shapes and frequencies and their impact upon aeroelastic characteristics of lifting surfaces; and, the identification of a parameter set that is useful for preliminary aeroelastic design.

Presented as Paper 83-0961-CP at the AIAA/ASME/ASCE/AHS Structures, Structural Dynamics, and Materials Conference, Lake Tahoe, Nev., May 2-4, 1983; received Aug. 8, 1983; revision received July 20, 1984.

*Professor, School of Aeronautics and Astronautics. Member AIAA.
†Engineer II, Advanced Systems Division. Member AIAA.

Mathematical Models for Anisotropic Beam Stiffness

In aeronautical preliminary design, the deflection characteristics of a slender beam or tube are useful to the understanding and study of bend/twist features of actual lifting surfaces with moderate-to-high aspect ratio. One method of characterizing the cross-sectional stiffness characteristics and the resulting coupled deflection behavior of an anisotropic laminated beam is proposed in Ref. 11. This idealization describes the coupled bend/twist behavior of a straight laminated beam by defining three beam cross-sectional stiffness parameters along a spanwise midsurface reference axis. This reference axis is chosen so that, without bend/twist cross coupling, it would correspond to the elastic axis of a similar orthotropic structure. These parameters are: EI, a bending stiffness parameter; GJ, a torsional stiffness parameter; and, a bend/twist coupling parameter, K.

At any cross section on the beam (see Fig. 1), the relationship between the internal bending moment resultant M, torque T, and the beam curvature $\partial^2 h/\partial_y^2$, and twist rate $\partial\alpha/\partial_y^2$, may be expressed as

$$\begin{Bmatrix} M \\ T \end{Bmatrix} = \begin{bmatrix} EI & -K \\ -K & GJ \end{bmatrix} \begin{Bmatrix} h'' \\ \alpha' \end{Bmatrix} \tag{1}$$

The notation $(\ )'$, refers to differentiation with respect to y. In turn, a flexibility relationship may be written as

$$\begin{Bmatrix} h'' \\ \alpha' \end{Bmatrix} = \frac{1}{1-kg} \begin{bmatrix} & g/EI \\ g/EI & 1/GJ \end{bmatrix} \begin{Bmatrix} M' \\ T \end{Bmatrix} \tag{2}$$

where $g = K/GJ$ and $k = K/EI$.

The ratio of the resultant bending moment M to spanwise curvature h'' is found to be

$$M/h'' = EI(1-kg) = EI_E \tag{3}$$

A common measure of "bending stiffness" is this ratio of M/h'' in Eq. (3). Similarly, the effective torsional stiffness GJ_E may be defined as

$$GJ_E = T/\alpha' = GJ(1-kg) \tag{4}$$

Although K may be either positive or negative, the product $kg = K^2/EIGJ$ is always positive. This means that "bending stiffness" and "torsional stiffness" decrease with increased coupling K if EI and GJ are held constant. These effective cross-sectional stiffnesses are often referred to as "free" values of these parameters since both bending and twisting occur. The parameters EI and GJ may be regarded as the "pure" stiffness parameters since, if only one mode of deformation is allowed at a time, (h'' or α' zero), EI and GJ will then be the effective stiffnesses (cf., Ref. 2).

One important feature of the presence of stiffness cross coupling is that the terms "bending stiffness" and "torsional stiffness" [as defined in Eqs. (3) and (4)] must be used with caution. For this reason, the term EI, as it appears in Eq. (1), will be referred to as the bending stiffness *parameter*, while the term GJ is termed the torsional stiffness *parameter*. Only when $K=0$ are these parameters equivalent to the physical measures of bending and torsional stiffness given in Eqs. (3) and (4).

Because strain energy considerations require the term $(1-kg)$ to be greater than zero, kg (a nondimensional product) must take on values between zero and unity. This nondimensional product may be expressed in terms of a parameter, ψ, defined by the relationship

$$\psi^2 = K^2/EI\ GJ < 1 \tag{5}$$

or

$$-1 < \psi < 1 \tag{6}$$

Niblett[12] has defined a similar "cross-flexibility" parameter with the same limits as ψ. Notice that, if the resultant torque is zero, then, for a given bending moment M, we have, from Eq. (2),

$$\left(\frac{\alpha'}{h''}\right)_{T=0} = g \tag{7}$$

Also, if M is zero, then, for a given torque T,

$$\left(\frac{h''}{\alpha'}\right)_{M=0} = k \tag{8}$$

Combining Eqs. (7) and (8), we have the following relationship:

$$\left(\frac{\alpha'}{h''}\right)_{T=0} = \left(\frac{K^2}{EI\ GJ}\right)\left(\frac{\alpha'}{h''}\right)_{M=0} = \psi^2\left(\frac{\alpha'}{h''}\right)_{M=0} \tag{9}$$

Equation (9) provides an additional indication of the limits of the stiffness cross-coupling parameter ψ, since the twist rate α' caused by a bending moment cannot exceed that caused by a twisting moment. The limits of the ratio $\psi = K/\sqrt{EI\ GJ}$ enable one to categorize a beam-like structure as highly coupled or lightly coupled, with values near zero categorized as lightly coupled, while absolute values of ψ near unity are associated with highly coupled structures.

Without an actual structure on which to conduct experiments, one can only determine the probable effects of cross-coupling through abstract mathematical models. In this paper, such beam models are divided into three classes:

1) High-aspect-ratio plates in which the chordwise bending moment is neglected in comparison to the spanwise moment.

2) A chordwise-rigid plate in which rib-like stiffners provide total restraint against camber bending (chordwise curvature is zero).

3) An anisotropic, thin-wall tube for which classical concepts such as shear flow are used to compute torsional stiffness.

A High-Aspect-Ratio Plate Model

Let us first consider a beam model based upon laminated plate theory. In the case of a midsurface symmetric plate, the relationship between plate bending moments, twisting moment, and curvatures may be expressed as (see, for example, Ref. 13):

$$\begin{Bmatrix} M_x \\ M_y \\ M_{xy} \end{Bmatrix} = \begin{bmatrix} D_{11} & D_{12} & D_{16} \\ D_{12} & D_{22} & D_{26} \\ D_{16} & D_{26} & D_{66} \end{bmatrix} \begin{Bmatrix} \kappa_x \\ \kappa_y \\ \kappa_{xy} \end{Bmatrix} \tag{10}$$

The elements D_{ij} are anisotropic plate stiffness constants that are functions of laminate ply geometry, material properties, and stacking sequence, while κ_x, κ_y, and κ_{xy} are plate curvatures.

If we adopt the y axis in Fig. 1 as a reference axis, the plate deflection $w(x,y)$ and the beam deflection $h(y)$ and twist $\alpha(y)$ are defined as

$$h(y) = w(0,y) \tag{11}$$

and

$$\left.\frac{\partial w}{\partial x}\right|_{x=0} = -\alpha(y) \tag{12}$$

In this case. we approximate the plate curvatures as follows:

$$\kappa_y \cong -h'' \tag{13}$$

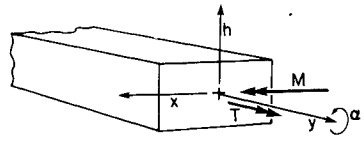

Fig. 1 Beam reference axis deformations, cross-sectional force, moment resultants and geometry.

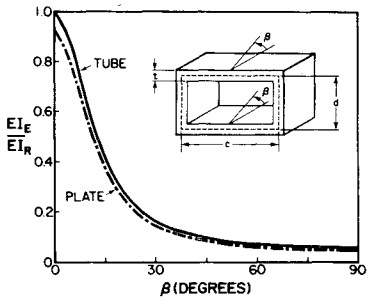

Fig. 2 Effective bending stiffness EI_E vs ply orientation β for both the plate model and thin-wall tube model with unidirectional laminates; $d/c = 0.25$, $t/d = 0.025$.

and

$$\kappa_{xy} \cong 2\frac{\partial^2 w}{\partial x \partial y}\bigg|_{x=0} = -2\alpha' \tag{14}$$

The relationships between moment resultants on the beam and those on the plate cross section (as defined in Ref. 13) are found to be

$$M = -M_y c \tag{15}$$

$$T = 2cM_{xy} \tag{16}$$

If the chordwise moment M_x is assumed to be zero, then Eq. (10) may be condensed to the following form:

$$\begin{Bmatrix} M \\ T \end{Bmatrix} = c \left[\begin{array}{c|c} \left(D_{22} - \frac{D_{12}^2}{D_{11}}\right) & -2\left(D_{26} - \frac{D_{16}D_{12}}{D_{11}}\right) \\ \hline -2\left(D_{26} - \frac{D_{16}D_{12}}{D_{11}}\right) & 4\left(D_{66} - \frac{D_{16}^2}{D_{11}}\right) \end{array}\right] \begin{Bmatrix} h'' \\ \alpha' \end{Bmatrix} \tag{17}$$

A term-by-term comparison between Eqs. (17) and (1) shows that

$$EI = c\left(D_{22} - \frac{D_{12}^2}{D_{11}}\right) \tag{18}$$

$$K = 2c\left(D_{26} - \frac{D_{12}D_{16}}{D_{11}}\right) \tag{19}$$

$$GJ = 4c\left(D_{66} - \frac{D_{16}^2}{D_{11}}\right) \tag{20}$$

Equations (3-6) and (18-20) may be used to compute the effective bending and torsional stiffnesses and the cross-coupling parameter ψ once the laminate geometry is defined.

Although Eqs. (13) and (14) have been used as approximations to the plate curvatures so that the two-dimensional plate model can be reduced to a one-dimensional beam model, note that chordwise curvature κ_x or "camber" bending has not been restrained. We now turn to a slightly different model in which camber bending is restrained to be zero.

A Chordwise-Rigid Laminated Plate Model

In aeroelastic work, chordwise rigidity is often assumed when stiff, closely spaced ribs are present within a wing of moderate-to-high aspect ratio. When this is the case, a slightly different stiffness model, also based upon laminated plate bending theory, can be used to predict anisotropic beam stiffness. To develop this model, the following assumed displacement state is used for plate deflection, $w(x,y)$:

$$w(x,y) = h(y) - x\alpha(y) \tag{21}$$

This approach, applied to orthotropic laminates, was originally suggested by Stein and Housner[14] and has been adapted to symmetrical, unbalanced laminated plates.[11]

This plate deflection approximation results in the following expressions for plate curvatures:

$$\kappa_x = 0 \tag{22}$$

$$\kappa_y = -h'' \tag{23}$$

$$\kappa_{xy} = -2\alpha' \tag{24}$$

Thus, the chordwise moment M_x is not zero, but, instead, is given by

$$M_x = -D_{12}h'' - 2D_{16}\alpha' \tag{25}$$

The stiffness parameters for the chordwise rigid laminated plate (CRLP) model are then found from Eq. (10) to be

$$EI = cD_{22} \tag{26}$$

$$GJ = 4cD_{66} \tag{27}$$

$$K = 2cD_{26} \tag{28}$$

Comparing Eqs. (26-28) with Eqs. (18-20), we see that only in the limit as D_{11} tends to infinity (infinite chordwise rigidity) are the two models identical.

A Laminated Tube Model

Both of the previously described laminated plate models have deficiencies because neither can account for flexible transverse shear webs as are present in box-beam design. This is a potentially important deficiency because of the widespread use of thin-wall, single- and multicell torque boxes in airplane design.

Mansfield and Sobey[15] have suggested a mathematical model for laminated composite, thin-wall, beam stiffness analysis. Reference 15 presents a derivation of the expressions for the coupled flexural, torsional, and extensional stiffness of a thin-wall, single-cell, laminated composite beam. The theoretical development of Ref. 15 is lengthy and will not be retraced here; however, their theory will be used for comparison purposes in the examples to follow.

It is important to examine and compare the cross-sectional stiffness predictions of various beam models such as those previously described. Researchers at MIT[16-18] have shown that, using the Rayleigh-Ritz method, there may be substantial differences in predicted natural frequencies depending upon whether or not camber bending is included. Therefore, the two models based on plate theory need to be compared. But, because the physical structure may have flexible vertical webs, all three models should be examined. For these comparisons we will use the three models described previously to generate stiffness data and then compare results.

Example Case: A Thin-Wall Rectangular Tube

To illustrate some of the features of the three beam stiffness models, a thin-wall tube with a rectangular cross-sectional shape is considered. The ratio of tube depth d to width c is equal to 0.25. The ratio of wall thickness to depth is 0.025. The material is unidirectional graphite/epoxy, T3000. Although strength considerations would preclude the use of such a laminate in actual design, it represents a limiting case for this material. The tube has ply symmetry with respect to the x and y planes at the middle surface. An angle β measured from the y axis (in the x-y plane) identifies the ply orientation (see the insert in Fig. 2).

Figure 2 compares the effective bending stiffness EI_E vs fiber angle β for the plate and tube models. The CRLP bending stiffness is not shown since it is nearly identical to, although slightly larger than, the plate model prediction. Because the bending stiffness is symmetrical about $\beta = 0$, only the range 0 deg $\leq \beta \leq 90$ deg is shown. Bending stiffness data has been normalized with respect to the quantity EI_R, the effective bending stiffness of the tube model with $\beta = 0$. From Fig. 2 it is seen that the plate model slightly underestimates the bending stiffness when compared to the tube model.

Significant differences in the values of ψ predicted by the three models are apparent from an examination of Fig. 3.

Note that ψ is an antisymmetrical function of β. The maximum value of the cross-coupling parameter predicted by the CRLP model is greater than either the tube or plate model and occurs at a somewhat larger value of β.

In Fig. 4, predicted values of effective torsional stiffness, GJ_E, for each of the three theories are compared; GJ_R is the value of effective torsional stiffness for the tube with $\beta=0$. The stiffness GJ_E is symmetrical about $\beta=0$. Because only the tube has vertical web shear flexibility, the tube theory predicts smaller torsional stiffnesses than either the plate model or CRLP laminated beam model. The maximum torsional stiffness for the tube occurs near $\beta=40$ deg, while for the plate it occurs at 45 deg. The CRLP theory predicts that the maximum effective torsional stiffness will occur near $\beta=65$ deg.

The differences between the computed torsional stiffness of the models can be attributed to the fact that the tube model has flexible vertical shear webs, while the beam and plate models assume transverse shear rigidity. This latter assumption is equivalent to assuming infinitely stiff (in shear) vertical webs. Therefore, the torsional stiffness predicted by tube theory should be less than that predicted by either the laminated beam model or the plate model for an identical cross-section geometry. Bredt's formula for an isotropic material predicts the ratio of GJ_f (the effective torsional rigidity of the rectangular cross-section tube with flexible shear webs) to GJ_r (the torsional rigidity of a similar tube with rigid vertical webs) to be

$$\frac{GJ_f}{GJ_r}=\frac{1}{1+d/c} \tag{29}$$

As the cross section changes from a square ($d/c=1$) to a thin rectangle ($d/c\ll 1$), the torsional stiffness predicted by each model will approach each other, as illustrated in Ref. 19.

These results indicate that caution must be exercised when choosing a model for laminated beam stiffness behavior. Unless one is very sure that the assumption of chordwise rigidity is satisfied, the plate model appears to be a better choice than the CRLP model. For thin-wall beam cross sections, where the width-to-depth ratio is large, there will be little difference between the results predicted by tube and plate theories. When this is the case, plate theory is preferable because it is simpler to apply.

Fortunately, for bend/twist coupling in actual designs, the greatest aeroelastic tailoring benefits are usually achieved when the tailored fibers (the β fibers) are relatively near $\beta=10$ deg. All three models produce similar results in this region. In addition, results indicate that chordwise stiffness, such as might be produced by ribs, or chordwise plies, may be advantageous if large values of stiffness cross coupling are required.

Free Vibration of Beams with Bend/Twist Cross-Coupling

The presence of stiffness cross-coupling in a beam-like structure can provide large changes in both the frequencies and mode shapes of similar, but orthotropic, laminates. To investigate the behavior of mode shapes and frequencies as a function of laminate cross-coupling, a beam finite element, including stiffness cross-coupling, was developed.[19] This element uses the static deformation of a beam with concentrated loads applied to its ends as the shape function for the strain energy and kinetic energy expressions used to develop the element stiffness and mass matrices.

One important effect of bend/twist elastic coupling is to modify any inertial cross-coupling due to static unbalance of a

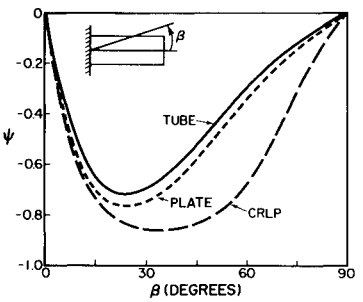

Fig. 3 Cross-coupling parameter ψ vs ply orientation β for the three beam models. Unidirectional laminate; $d/c=0.25$, $t/d=0.025$.

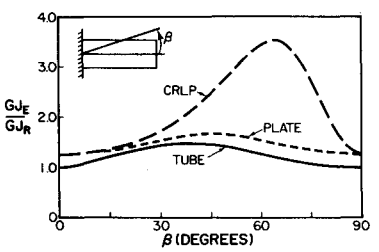

Fig. 4 Effective torsional stiffness GJ_E vs ply orientation β for the three beam models. Unidirectional laminate; $d/c=0.25$, $t/d=0.025$.

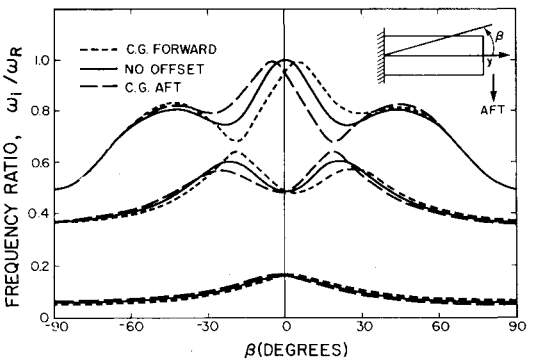

Fig. 5 Effect of ply angle β upon the first three natural frequencies of a laminated beam. Three c.g. positions are shown; β plies comprise 65% of the laminate.

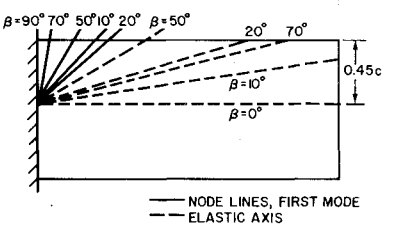

Fig. 6 Node line positions for the fundamental vibration mode of a laminated beam together with elastic axis positions for several values of ply orientation, β.

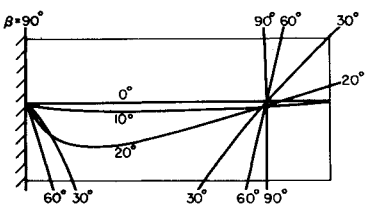

Fig. 7 Node line positions for the second normal mode of a laminated beam for several values of ply orientation, β.

lifting surface. Since "mass balancing" or positioning of the wing cross-sectional centers of mass is one commonly used method of raising the flutter speed of an airfoil, it is of interest to determine how we can use "elastic balancing" or tailoring to achieve the same objective. An example will serve to illustrate the potential for the use of laminate tailoring to modify free-vibration characteristics of cross-coupled beam-like structures.

The example chosen for this illustration is an unswept cantilever beam whose stiffness is entirely due to laminated cover skins. The beam has a span of 160 in., a structural chord of 24 in., and an aerodynamic chord of 72 in. Symmetrical laminated cover skins have 65% of their fibers oriented at an angle β to a spanwise structural reference axis while 25% are oriented at ± 45 deg and the remaining 10% at $\beta = 90$ deg. The CRLP theory is used to compute all cross-sectional stiffness parameters. This laminate is moderately coupled in the range 15 deg $< \beta <$ 55 deg. The cross coupling reaches a maximum of $\psi = 0.68$ near $\beta = 30$ deg. A finite element analysis using beam elements with stiffness cross coupling included was used to determine the natural frequencies of the beam as a function of the ply angle β.

Figure 5 displays the first three beam natural frequencies as a function of β. These frequencies are referenced to the third natural frequency, computed when $\beta = 0$ deg. In addition to a case with no inertia unbalance, two values of static unbalance, measured as the distance between the line of centers of mass and the reference axis, were considered. With no static unbalance the behavior of the frequencies with β is symmetrical about $\beta = 0$ deg. The frequency of the fundamental mode declines as β increases from 0 deg and is primarily dependent upon the effective bending stiffness. The frequency of the second mode first increases with β and then declines. At $\beta = 0$ deg, this mode is identified with the first torsional mode. As β increases from zero, so too does the effective torsional stiffness. The frequency of the third mode decreases with increasing β in the vicinity of $\beta = 0$ deg, and is the second bending mode at $\beta = 0$ deg.

Stiffness cross-coupling between bending and torsional deformation and the declining value of EI_E and increasing values of GJ_E as β increases cause the natural frequencies of modes 2 and 3 to approach each other in the vicinity of $\beta = 20$ deg (and $\beta = -20$ deg). This same phenomenon was first observed by Ritchie and Rosinger[6] and later by Jensen.[17] Ritchie and Rosinger note that frequency merging is precluded when the effect of cross-coupling is included in the stiffness model. However, as β increases from $\beta = 0$ deg, the original uncoupled (or, in the case of inertia unbalance, nearly uncoupled) modes become coupled to the extent that, while their frequencies do not merge, they actually interchange their shapes. This "modal transfer" phenomenon is best seen by examining the deflected shapes of the beam vibrating in each of its normal modes. It is to this examination that we now turn.

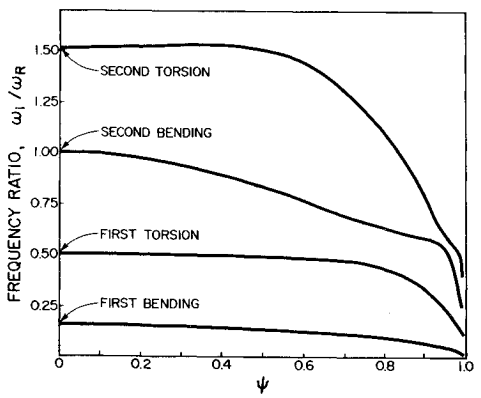

Fig. 8 Effect on the natural frequencies of an example beam caused by changing the stiffness cross-coupling, ψ. The ratio $R = GJ/EI$ is fixed at $R = 0.5$.

The Effect of Stiffness Cross-Coupling on Normal Mode Shapes

The elastic axis of a beam may be defined as the locus of points (in the x-y coordinate system) at which a transverse force may be applied and cause only bending and no twist (about the y axis) *on the section on which the force is applied.* It can be shown that, in the case of a uniform laminated beam, this elastic axis is a straight line whose orientation angle γ with respect to the reference axis (γ is positive counterclockwise when viewed from above) is given by

$$\gamma = \tan^{-1}\left(\frac{-K}{2EI}\right) = \tan^{-1}\left(\frac{-\psi\sqrt{R}}{2}\right) \tag{30}$$

where

$$R = GJ/EI \tag{31}$$

Since negative K and ψ values are associated with forward swept ($\beta > 0$) plies, the angle γ follows the β orientation of the "tailored" plies. Elastic axis positions for four values of β are shown in Fig. 6 for this example. Note that K/EI reaches its maximum value near $\beta = 50$ deg in this case.

Also plotted in Fig. 6 are node lines, for the same four values of β, associated with the fundamental mode of vibration of the beam. When β is equal either to 0 or 90 deg, this node line lies along the fixed root support. However, as the β ply rotates forward from $\beta = 0$, the node line first rotates outboard from the support and then rotates back parallel to the support when $\beta = 90$ deg. From a structural standpoint, the appearance of the node line in these inclined positions is similar to sweeping the root fixity clockwise in Fig. 6. Note also that repositioning the line of sectional centers of mass *aft*

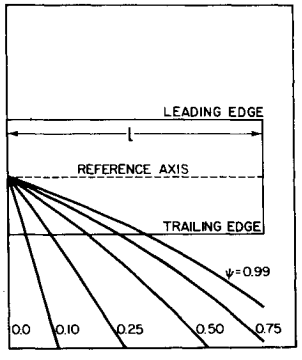

Fig. 9 Effect of the parameter ψ upon the node line position for the fundamental mode of vibration. The ratio $R = GJ/EI$ is fixed at $R = 0.5$.

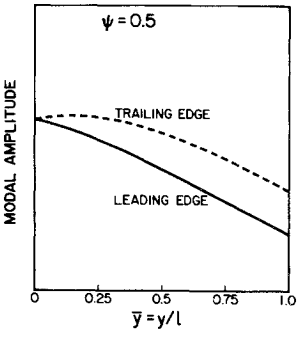

Fig. 10 Edge view of cantilever beam vibration mode shape; fundamental mode with $\psi = 0.5$ and $R = 0.5$.

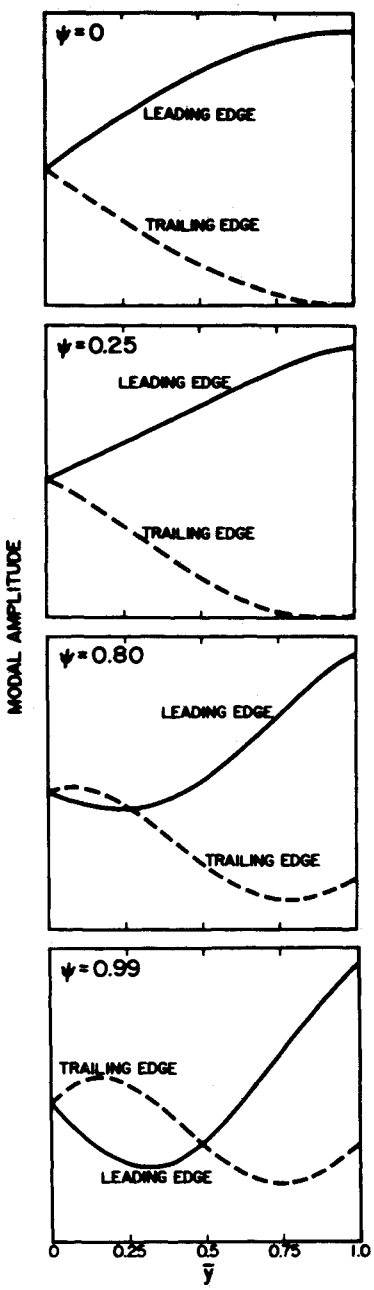

Fig. 11 Straight-on view of the example beam second mode shape for four values of ψ. $R=0.5$. Note that boundary conditions are applied along the reference axis, not the leading and trailing edges.

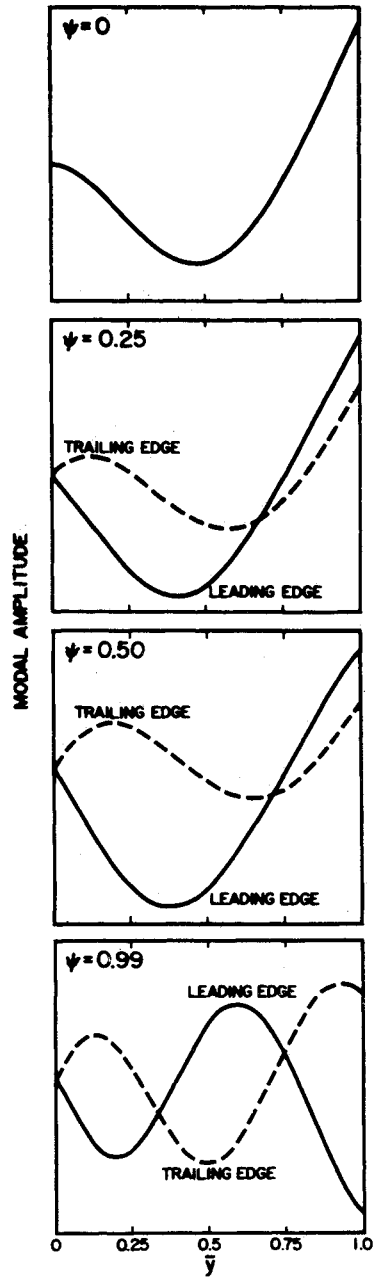

Fig. 12 Straight-on view of the example beam third mode shape for four values of ψ. $R=0.5$.

of the reference axis will cause a similar node line rotation for this mode.

A plot of node line positions, associated with the second mode of vibration, is shown in Fig. 7 for several values of β. It is seen that, at $\beta=0$ deg, this mode is a pure torsion mode, as evidenced by a node line located along the reference axis. As β increases from zero, the initially straight node line curves aft, as indicated by the node lines when $\beta=10$ and 20 deg. At β values above 25 deg, the curvature of the node line is so extreme that portions of the curves are off the scale used in Fig. 7. Finally, at $\beta=90$ deg, two parallel node lines appear, one along the root support and the other passing through a point at about 0.8 of the span. Thus the second mode begins as first torsion and, through an evolutionary process, transmutes to become the second bending mode.

The three parameters, EI, GJ, K, that characterize the cross-sectional stiffness of a cross-coupled beam may be combined to yield two nondimensional parameters. One parameter is ψ, the cross-coupling parameter, while the other is $R=GJ/EI$. With laminated beams, both ψ and R change with changes in ply orientation. Thus, the previous examples illustrating the effects of ply orientation on natural frequency and node line position contain both the effect of the change in stiffness ratio R and cross-coupling parameter ψ.

To illustrate the effects on free vibration of a change only in cross-coupling ψ, while holding R and GJ fixed, consider the example of a beam with a planform identical to that used in the previous study, and a ratio $R=GJ/EI$ equal to 0.5. Inertial parameters are also the same as in the previous example.

Figure 8 shows the nondimensional values of the first four cantilever beam natural frequencies as a function of ψ. Ten finite elements were used in these calculations. At $\psi=0$, the ordering of these frequencies is: first bending, first torsion, second bending, second torsion. Except for the third natural frequency, the natural frequencies are relatively unaffected by changes in ψ until $\psi=0.40$. Figure 9 presents a sequence of

node line positions for the first mode as ψ changes. Figure 10 shows an edge view of the beam leading and trailing edges in the fundamental mode as it would appear in a downstream view when $\psi = 0.5$. Strong coupling between bending and torsional deformation is seen to be present.

Figure 11 shows a sequence of mode shape changes for the second normal mode at selected values of ψ. The transmutation of this mode from first torsion to a highly coupled mode resembling second torsion is evident. Finally, Fig. 12 shows the changes in the third mode as ψ changes. This mode begins as second bending and evolves into a mode that closely resembles an uncoupled third torsion mode. From these examples, it is seen that stiffness cross coupling between bending and twisting deflections has a substantial effect on the mode shapes, but a lesser effect on natural frequency unless the laminate is highly coupled. The important parameter in this process appears to be the cross-coupling parameter, ψ.

Conclusion

Several issues related to preliminary analysis and design of high-aspect-ratio, beam-like surfaces have been identified and illustrated. Chordwise stiffness has been shown to have a significant influence on the amount of bend/twist cross coupling. A cross-coupling parameter ψ is suggested as a measure of the elastic bend/twist coupling present in a beam-like structure. The influence of this parameter upon the free-vibration mode shapes is found to be substantial. This influence suggests its use as a modal coupler/decoupler. In addition, the use of nondimensional parameter combinations such as ψ and R for design tradeoff studies may prove useful since the laminate geometry and internal construction details need not be defined for such a study.

Finally, it should be noted that tailoring principles are not restricted merely to advanced composite materials. While composite materials offer an efficient, effective method of introducing cross-coupling between structural degrees of freedom, one may also use other methods of obtaining directional stiffness (see, for example, Ref. 20). The increased modal participation or "modal activity" generated by cross coupling might, for instance, have a beneficial effect upon the amount of structural damping in a particular mode. This might prove useful in the design of some large space structures. However, whether it be for aeroelastic or astroelastic purposes, the exploitation of directional stiffness properties represents a potentially useful tool to add to the myriad of design options available to the designer.

Acknowledgments

This work was supported, in part, by the Naval Air Systems Command under Contract NO19K0194 and by NASA Langley Research Center under Grant HSG-1-157.

The first author wishes to acknowledge the research assistance of Mr. Steven Stukel, formerly a graduate student at Purdue. Thanks also go to Prof. C. W. Bert of the University of Oklahoma for his gracious assistance in uncovering several valuable archival references.

References

[1] Voight, W., *Lehrbuch der Kristallphysik*, Teubner, Leipzig, 1928.

[2] Brown, W. F. Jr., "Interpretation of Torsional Frequencies of Crystal Specimens," *Physical Review*, Vol. 58, Dec. 1940, pp. 998-1001.

[3] Hearmon, R. F. S., "The Significance of Coupling Between Shear and Extension in the Elastic Behavior of Wood and Plywood," *Proceedings of the Physics Society*, Vol. 55, 1943, pp. 67-80.

[4] Abarcar, R. B. and Cunniff, P. F., "The Vibration of Cantilever Beams of Fiber Reinforced Material," *Journal of Composite Materials*, Vol. 6, Oct. 1972, pp. 504-517.

[5] Clary, R. R., "Vibration Characteristics of Unidirectional Filamentary Composite Material Panels," *Composite Materials: Testing and Design (Second Conference)*, ASTM STP 497, 1972, pp. 415-438.

[6] Ritchie, I. G. and Rosinger, H. E., "Torsion-flexure Coupling in a Composite Material," *Journal of Physics (D): Applied Physics*, Vol. 7, No. 9, June 1974, L95.

[7] Ritchie, I. G., Rosinger, H. E., Shillinglaw, A. J., and Fleury, W. H., "The Dynamic Elastic Behavior of a Fibre-Reinforced Composite Sheet: I. The Precise Experimental Determination of the Principal Elastic Moduli," *Journal of Physics (D): Applied Physics*, Vol. 8, No. 15, Oct. 1975, pp. 1733-1749.

[8] Ritchie, I. G., Rosinger, H. E., and Fleury, W. H., "The Dynamic Elastic Behavior of a Fibre-reinforced Composite Sheet: II. The Transfer Matrix Calculation of the Resonant Frequencies and Vibration Shapes," *Journal of Physics (D): Applied Physics*, Vol. 8, No. 15, Oct. 1975, pp. 1750-1768.

[9] Wallace, M. M. and Bert, C. W., "Transfer Matrix Analysis of Dynamic Response of Composite-Material Structural Elements with Material Damping," *Shock and Vibration Bulletin*, Vol. 50, Pt. 3, Sept. 1980, pp. 27-37.

[10] Shirk, M. H., Hertz, T. J., and Weisshaar, T. A., "A Survey of Aeroelastic Tailoring: Theory, Practice, Promise," AIAA Paper 84-0982, May 1984.

[11] Weisshaar, T. A., "Aeroelastic Stability and Performance Characteristics of Aircraft with Advanced Composite Sweptforward Wing Structures," AFFDL-TR-78-116, June 1978.

[12] Niblett, L. T., "Divergence and Flutter of Swept-forward Wings with Cross-Flexibilities," Royal Aircraft Establishment TR 80047, April 1980.

[13] Tsai, S. W. and Hahn, H. T., *Introduction to Composite Materials*, Technomic Publishing Co., Westport, Conn., 1980.

[14] Stein, M. and Housner, J. G., "Flutter Analysis of Swept-Wing Subsonic Aircraft with Parameter Studies of Composite Wings," NASA TN D-7539, Sept. 1974.

[15] Mansfield, E. H. and Sobey, A. J., "The Fiber Composite Helicopter Blade," *Journal of the Royal Aeronautical Society*, Vol. XXX, Pt. 2, May 1979, pp. 413-449.

[16] Crawley, E. F. and Dugundji, J., "Frequency Determination and Nondimensionalization for Composite Cantilever Plates," *Journal of Sound and Vibration*, Vol. 72, No. 1, 1980, pp. 1-10.

[17] Jensen, D. W., Crawley, E. F., and Dugundji, J., "Vibration of Cantilevered Graphite/Epoxy Plates with Bending-Torsion Coupling," *Journal of Reinforced Plastics and Composites*, Vol. 1, July 1982, pp. 254-269.

[18] Hollowell, S. J. and Dugundji, J., "Aeroelastic Flutter and Divergence of Stiffness Coupled, Graphite-Epoxy, Cantilevered Plates," *Proceedings of the 23rd AIAA Structures, Structural Dynamics and Materials Conference*, May 1982, pp. 416-426.

[19] Weisshaar, T. A., "Structural Dynamic Tailoring of Advanced Composite Lifting Surfaces," School of Aeronautics and Astronautics, Purdue University, W. Lafayette, Ind., TR-AAE-82-1, June 1982.

[20] Gratke, S. D. and Williams, J. G., "Analysis/Theory of Controlled Configured Structure (CCS)," AIAA Paper 77-1212, Aug. 1977.